Heliyon 10 (2024) e34056

Contents lists available at ScienceDirect

Heliyon

journal homepage: www.cell.com/heliyon

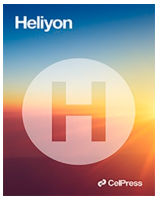

Research article

Thermal analysis of radiative Sutterby nanofluid flow over stretching curved surface

Nadeem Abbas [a], Wasfi Shatanawi [a,b,c,*], Fady Hasan [a], Zead Mustafa [b]

[a] Department of Mathematics and Sciences, College of Humanities and Sciences, Prince Sultan University, Riyadh, 11586, Saudi Arabia
[b] Department of Mathematics, Faculty of Science, The Hashemite University, P.O Box 330127, Zarqa, 13133, Jordan
[c] Department of Medical Research, China Medical University Hospital, China Medical University, Taichung, 40402, Taiwan

ARTICLE INFO

Keywords:
Sutterby fluid
Buongiorno model
Radiation
Curved surface
Slip effects

ABSTRACT

In this analysis, Sutterby fluid model over a curved surface is considered. The main mechanisms that contribute to the improvement of the convection characteristics of the nanofluid are categorized as Brownian motion and thermophoresis. The radiation and slip mechanism have been studied at curved stretchable surface. The suction/injection impacts also studied. The partial differential equations are converted into ordinary differential equations through transformations.

The numerical solution of the specified mathematical model is obtained using the built-in bvp4c tool in MATLAB. The effects of various parameters related to the system of ordinary differential equations are illustrated in the graphs. The influence of some intended parameters through the physical quantities are presented through tabular form.

Nomenclature

ω	Section/injection parameter	N_B	Brownian motion
R_d	Radiation	ϖ	Sutterby fluid
δ	Thermal slip	ς	Curvature
δ_1	Concentration slip	Ec	Eckert number
∇	Gradient operator	ρ_f	Density of fluid
μ_f	Dynamic viscosity	$(C_p)_f$	Fluid heat capacity
$K(T)$	Variable thermal conductivity	$(C_p)_s$	Heat capacity of particle
ρ_s	Density of particles	T	Temperature
C	Concentration	T_∞	Temperature of Ambient
C_∞	Concentration of Ambient	D_B	Brownian diffusion
D_T	Thermophoretic	B	Dipole of Magnetic
E_c	Activation energy dimensionless	Pr	Prandtl number

1. Introduction

The fact that non-Newtonian fluids are presented in real life which has led to some applications in the engineering, biological, pharmaceutical, and industrial fields. The rheological properties of complex fluid models are paints, industrial oils, polymeric

* Corresponding author. Department of Mathematics and Sciences, College of Humanities and Sciences, Prince Sultan University, Riyadh, 11586, Saudi Arabia.
E-mail address: wshatanawi@psu.edu.sa (W. Shatanawi).

https://doi.org/10.1016/j.heliyon.2024.e34056
Received 12 July 2023; Received in revised form 15 June 2024; Accepted 3 July 2024
Available online 4 July 2024

solutions, and so on belong to the power-law fluid model. For the first time, Sutterby [1] initiated the idea to combine study of dilatant and pseudoplastic fluid properties. This idea has attracted much attention from researchers due to its several applications in real-life problems. The uses of such types of fluids played an essential role in engineering and industries. Akbar and Nadeem [2] prolonged the ideas of Sutterby [1] for peristaltic model having asymmetric channel inclindely. The analytical results have developed to present the effects of slip. Ahmad et al. [3] disputed the flow of Sutterby fluid analytically. The impact of chemical, radiation, and mixed convection on a squeezed channel are considered. Khan et al. [4] considered the reaction of heterogeneous-homogeneous on Sutterby fluid at a rotating desk. The Cattaneo–Christov model is executed on the Sutterby fluid model to attain the major results. Sajid et al. [5] reflected the Maxwell Sutterby fluid flow at an inclined exponential stretching surface. The MHD impacts with temperature-dependent properties have been studied in their analysis. Activation energy and heat sink/source influence have been debated on the exponential stretching surface. Mabood et al. [6] contested the dynamic characteristic of Sutterby fluid with Fourier and Fick law at spinning stretching disk. Abdal et al. [7] initiated to analyze the nanobioflim by Sutterby fluid at stretching sheet. Hanif et al. [8] tinted the model of Sutterby fluid. Hussain et al. [9] considered the Sutterby fluid the impressions of ferromagnetic field and magnetic dipole. Hussain et al. [10] contested the inspiration of Sutterby fluid flow model under the activation energy. Abdelsalam et al. [11] scrutinized the effects of Sutterby fluid in the occurrence of an entropy model. Recently, few authors have developed ideas about the Sutterby fluid model using various assumptions and stretchable surfaces (see Refs. [12,13]).

The boundary layer flow under the stretching of surface has been discussed in detail due to the number of applications in the real fields but stretchable sheets have one of the most important examples of procedure of manufacturing. Several types of stretching velocities are defined namely: nonlinear, linear, and exponentially stretching velocities. Several stretching velocities applications are hot rolling, glass blowing, rubber sheet, the product of paper, spinning of fiber, fiberglass, polymer sheet, and so on. In the early times, the boundary layer flow at stretchable surface was studied by Crane [14]. Crane [14] considered the cylindrical moving surface and debated the impacts of fluid at motion or rest. The impact boundary layer at faraway and close to the orifice surface. Vajravelu and Cannon [15] worked on the Crane [14] assumptions. Vajravelu and Cannon [15] considered the nonlinear stretchable surface to develop the analytical results. Sajid et al. [16] considered the viscous model at curved surface. In the early times, the results have been achieved analytically. Abbas et al. [17] deliberated the results of PST and PHF at stretching curved surface. The MHD is applied to the normal flow of viscous fluid and analytical results are achieved. Akbar et al. [18] initiated the Eyring power fluid at a stretchable surface with MHD influence. Sanni et al. [19] pondered the numerical outcomes of the power law stretchable curved sheet. Saif et al. [20] deliberated the Jeffrey fluid model at a curved sheet. The Buongiorno model with heat generation is debated at a curved sheet. Kumar et al. [21] deliberate the nanomaterial flow over curved sheet. The thermal and viscous impacts have been considered in their exploration. Bhatti and Abdelsalam [22] highlighted the influence of stretching surface impacts using the ferromagnetic flow of nanofluid. Nawaz et al. [23] discussed the third-grade fluid model using the stretchable parallel surface for mixed convection. Abbas et al. [24] pondered the influence of the radiative flow of Sutterby fluid at a nonlinear stretchable cylinder. Few researchers have studied the curved sheet under several fluid models with external flow assumptions (see Refs. [25–27]).

Nanofluids is a new class that was just established. A nanofluid is made up of base fluid with nanosized particles. The field of nanotechnologies and others benefited greatly from this development. Buongiorno [28] was initiated the comprehensive analysis of the convective transport of nanofluid based at MIT (Massachusetts Institute of Technology). He considered the seven slip mechanisms between base fluid and nanoparticles having relative velocities. Two of them are the most important found such as thermophoresis and Brownian diffusion. Rana et al. [29] used the finite element technique to investigate the nanofluid at a stretching surface. The time-dependent flow of MHD (Magneto-hydro-dynamics) is debated in their analysis. Goyal and Bhargava [30] debated the viscoelastic fluid with the Buongiorno model at a stretchable sheet. Boundary layer flow of double-diffusive using the finite element technique to achieve the results. Akbar [31] highlighted the impact of the Buongiorno model and Sutterby fluid under the natural convection of peristaltic flow in a porous channel. Hayat et al. [32] considered the satterby nanofluid under the chemical reactive flow and heat absorption. Sohail and Naz [33] studied the sutterby nanofluid at a stretchable cylinder. Khan et al. [34] discussed the inspiration for the magnetized flow of nanofluid with sutterby fluid model at a wedge. Abdelsalam and Zaher [35] discussed the

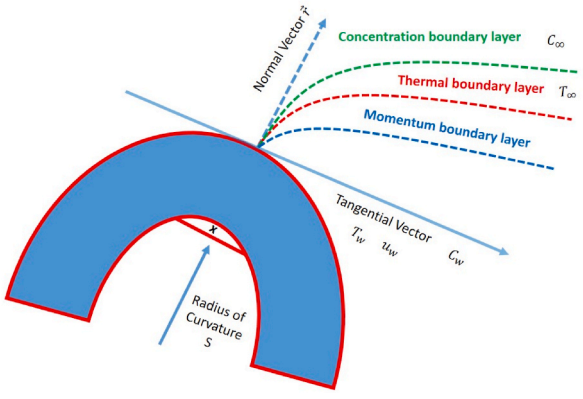

Fig. 1(a). Flow pattern of Sutterby nanofluid over stretching curved surface.

spermatic fluid in the attendance of electroosmotic forces. Aldabesh et al. [36] deliberated the inspiration of nanofluid under the microorganism phenomena. Nawaz et al. [37] discussed the heat transfer for micropolar fluid model. Few authors have developed ideas about the Buongiorno model under the flow mechanism (see Refs. [38–40]).

The literature presents an analysis of the Sutterby fluid model flowing over a curved surface, considering linear stretching velocity. The study includes the effects of suction/injection, Brownian motion, and thermophoresis on the curved surface. Thermal and concentration slip mechanisms are also accounted for. The mathematical model is cracked numerically by the bvp4c tool in MATLAB, and the impacts of various parameters related to the system of ordinary differential equations (ODEs) are reported in both graphical and tabular forms. The results illustrate how certain parameters influence physical quantities, making them applicable to real-life problems.

2. Mathematical formulation

Steady flow of incompressible sutterby nanofluid at stretchable curved surface which revealed in Fig. 1(a). Thermophoresis and Brownian motion mechanism are deliberated on the curved surface. Thermal and concentration slip mechanism is considered in present analysis. The fluid velocity invented as $u_w = ax$ (linear stretching) where $a > 0$ at curved surface. The (x,r) are the curvilinear coordinates and $x-$ along axial and $r-$ along radial directions. The radiation influence have been taken into account. The T_w (wall temperature) at surface and T_∞ (ambient temperature) is for away from surface. The C_w (wall concentration) at surface and C_∞ (ambient concentration) is for away from surface. S is the difference length between origin and surface such as the surface become flat if $S\to\infty$. The boundary approximation are implemented on the heat and mass transfer of Sutterby fluid and the physical model become in the differential form:

$$\frac{S}{S+r}\frac{\partial u}{\partial x}+\frac{1}{S+r}\frac{\partial}{\partial r}(v(r+S))=0, \tag{1}$$

$$\frac{u^2}{S+r}=\frac{1}{\rho_f}\frac{\partial p}{\partial r}, \tag{2}$$

$$\left(v\frac{\partial u}{\partial r}+\frac{Su}{S+r}\frac{\partial u}{\partial x}+\frac{vu}{S+r}\right)+\frac{1}{\rho_f}\frac{S}{S+r}\frac{\partial p}{\partial r}=\frac{\nu}{2}\left(\frac{\partial^2 u}{\partial^2 r}+\frac{1}{S+r}\frac{\partial u}{\partial r}-\frac{u}{(S+r)^2}-\frac{mN^2}{2}\left(\frac{\partial u}{\partial r}-\frac{u}{S+r}\right)^2\left(\frac{\partial^2 u}{\partial^2 r}-\frac{1}{3(S+r)}\frac{\partial u}{\partial r}+\frac{u}{3(S+r)^2}\right)\right), \tag{3}$$

$$\left(v\frac{\partial T}{\partial r}+\frac{Su}{S+r}\frac{\partial T}{\partial x}\right)-\frac{16\sigma^* T_m^3}{3k^*\rho C_p}\left(\frac{\partial^2 T}{\partial^2 r}+\frac{1}{S+r}\frac{\partial T}{\partial r}\right)=\alpha_f\left(\frac{\partial^2 T}{\partial^2 r}+\frac{1}{S+r}\frac{\partial T}{\partial r}\right)+\tau\left(D_B\left(\frac{\partial C}{\partial r}\right)\left(\frac{\partial T}{\partial r}\right)+\left(\frac{D_T}{T_\infty}\right)\left(\frac{\partial T}{\partial r}\right)^2\right)+\frac{\mu_0}{\rho C_p}\left(1-\frac{mN^2}{6}\left(\frac{\partial u}{\partial r}+\frac{u}{S+r}\right)^2\right)\left(\frac{\partial u}{\partial r}+\frac{u}{S+r}\right)^2, \tag{4}$$

$$\left(v\frac{\partial C}{\partial r}+\frac{Su}{S+r}\frac{\partial C}{\partial s}\right)-\left(\frac{D_T}{T_\infty}\right)\left(\frac{\partial^2 T}{\partial^2 r}+\frac{1}{S+r}\frac{\partial T}{\partial r}\right)=D_B\left(\frac{\partial^2 C}{\partial^2 r}+\frac{1}{S+r}\frac{\partial C}{\partial r}\right). \tag{5}$$

The respected boundary conditions are,

$$\begin{aligned} u=U_w+\lambda_2\left(\frac{\partial u}{\partial r}-\frac{u}{R+r}\right), v=V_w, T=T_w+\lambda_1\left(\frac{\partial T}{\partial r}\right), C=C_w+\lambda_0\left(\frac{\partial C}{\partial r}\right), at\ r\to 0,\\ u\to 0, \frac{\partial u}{\partial r}\to 0, T\to T_\infty, C\to C_\infty, \ at\ r\to\infty. \end{aligned} \tag{6}$$

The similarity variables are presented as

$$\begin{aligned} T=T_\infty+(T_w-T_\infty)\theta(\Upsilon), \Upsilon=\sqrt{\frac{a}{\nu_f}}r, u=axF'(\Upsilon),\\ v=-\frac{S}{r+S}\sqrt{a\nu_f}F(\Upsilon), C=C_\infty+(C_w-C_\infty)\varphi(\Upsilon), P=\rho a^2x^2p(\Upsilon). \end{aligned} \tag{7}$$

Eq. (7) of dimensionless terms are utilized on Eqs. (1)–(6) than become dimensionless form as:

$$P'=\frac{F'^2}{\Upsilon+\varsigma}, \tag{8}$$

$$\frac{2\varsigma}{\Upsilon+\varsigma}P=\left(\frac{1}{2}\right)\left[F'''+\frac{F''}{\Upsilon+\varsigma}-\frac{F'}{(\Upsilon+\varsigma)^2}\right]-\frac{\varsigma}{\Upsilon+\varsigma}F'^2+\frac{\varsigma}{\Upsilon+\varsigma}F'F''+\frac{\varsigma}{(\Upsilon+\varsigma)^2}FF'-\left(\frac{\varpi}{4}\right)\left(F''^2F'''-\frac{6F''F'''F'+F''^3}{3(\Upsilon+\varsigma)}-\frac{F'^2F''}{3(\Upsilon+\varsigma)^3}+\frac{F'^3}{3(\Upsilon+\varsigma)^4}+\frac{F''^2F'+F'^2F'''}{3(\Upsilon+\varsigma)^2}\right), \tag{9}$$

$$\frac{(1+R)}{Pr}\left(\theta''+\frac{1}{\Upsilon+\varsigma}\theta'\right)+\frac{\varsigma}{\Upsilon+\varsigma}F\theta'+(N_B\theta'\varphi'+N_T\theta'\theta')+Ec\left(F''^2-\frac{2F'F''}{\Upsilon+\varsigma}+\frac{F'^2}{(\Upsilon+\varsigma)^2}-\left(\frac{\varpi}{4}\right)\left(\frac{2F'^2F''^2}{(\Upsilon+\varsigma)^2}+F''^4+\frac{F'^4}{(\Upsilon+\varsigma)^4}-\frac{4F''^3F'}{\Upsilon+\varsigma}-4\frac{F'^3F''}{(\Upsilon+\varsigma)^3}+4\frac{F''^2F'^2}{(\Upsilon+\varsigma)^2}\right)\right)=0, \tag{10}$$

$$\left(\varphi''+\frac{1}{\zeta+K_0}\varphi'\right)+\frac{K_0}{\zeta+K_0}F\varphi'+\frac{N_B}{N_T}\left(\theta''+\frac{1}{\zeta+K_0}\theta'\right)=0, \tag{11}$$

The pressure profile can be computed from Eq. (9) as follows:

$$P(\zeta)=-\frac{F'}{4\varsigma(\Upsilon+\varsigma)^3}+\frac{F''}{4\varsigma}-\left(\frac{\varpi(\Upsilon+\varsigma)}{8\varsigma}\right)\left(F''^2F'''-\frac{F''^3+6F''F'''F'}{3(\Upsilon+\varsigma)}-\frac{F'^3}{3(\Upsilon+\varsigma)^4}-\frac{F'^2F''}{(\Upsilon+\varsigma)^3}+\frac{F'''F'^2+FF''^2}{(\Upsilon+\varsigma)^2}\right)+\left(\frac{(\Upsilon+\varsigma)}{2\varsigma}\right)\left(\frac{\varsigma\left(FF''-F'^2\right)}{(\Upsilon+\varsigma)}+\frac{\varsigma FF'}{(\Upsilon+\varsigma)^2}\right)+\left(\frac{(\Upsilon+\varsigma)}{4\varsigma}\right)F''', \tag{12}$$

Solving Eq. (8) and Eq. (12), while dismissing the term of pressure:

$$-\frac{F'-2\varsigma FF'}{(\Upsilon+\varsigma)^3}+F''''-\left(\frac{\varpi}{2}\right)\left(\frac{F'^2F''''+4F''F'''F'}{2}+F''^2F''''+2F'''^2F''-\frac{F'^3}{(\Upsilon+\varsigma)^5}-\frac{2F''^2F'''}{\Upsilon+\varsigma}-\frac{2F'^2F'''}{(\Upsilon+\varsigma)^3}-\frac{3F''^2F'}{(\Upsilon+\varsigma)^3}+\frac{3F'^2F''}{(\Upsilon+\varsigma)^4}+\frac{F''^3}{(\Upsilon+\varsigma)^2}-2\frac{FF''^2+F''''FF''}{\Upsilon+\varsigma}\right)+\frac{2F'''+2\varsigma(FF'''-F''F)}{\Upsilon+\varsigma}-\frac{2\varsigma F'^2+F''+2\varsigma FF''}{(\Upsilon+\varsigma)^2}=0, \tag{13}$$

$$\frac{1}{Pr}\left(1+\frac{4}{3}R_d\right)\left(\theta''+\frac{1}{\Upsilon+\varsigma}\theta'\right)+\frac{\varsigma}{\Upsilon+\varsigma}F\theta'+(N_B\theta'\varphi'+N_T\theta'\theta')+Ec\left(F''^2-\frac{2F'F''}{\Upsilon+\varsigma}+\frac{F'^2}{(\Upsilon+\varsigma)^2}-\left(\frac{\varpi}{4}\right)\left(\frac{2F'^2F''^2}{(\Upsilon+\varsigma)^2}+F''^4+\frac{F'^4}{(\Upsilon+\varsigma)^4}-\frac{4F''^3F'}{\Upsilon+\varsigma}-4\frac{F'^3F''}{(\Upsilon+\varsigma)^3}+4\frac{F''^2F'^2}{(\Upsilon+\varsigma)^2}\right)\right)=0, \tag{14}$$

$$\left(\varphi''+\frac{1}{\Upsilon+\varsigma}\varphi'\right)+\frac{\varsigma}{\Upsilon+\varsigma}F\varphi'+\frac{N_B}{N_T}\left(\theta''+\frac{1}{\Upsilon+\varsigma}\theta'\right)=0, \tag{15}$$

having boundary conditions are

$$\begin{aligned}&F(0)=\omega,F'(0)=1,\delta_1\varphi'(0)+1=\varphi(0),\\&\delta\theta'(0)+1=\theta(0),\theta(\infty)=F'(\infty)=\varphi(\infty)=F''(\infty)=0.\end{aligned} \tag{16}$$

The engineering quantities of the fluid flow at the surface are defined as:

$$C_f=\frac{\tau_{rx}}{\rho_f u_w^2},Nu_n=\frac{xq_w}{k_f(T_w-T_\infty)},Sh_n=\frac{xh_m}{D_B(C_w-C_\infty)}. \tag{17}$$

Where, the quantities (τ_{rs} and q_w) are revealed as

$$\tau_{rs}=\frac{\mu}{2}\left(1-\frac{mN^2}{6}\left(\left(\frac{u}{S+r}\right)^2-2\frac{1}{(S+r)}\frac{\partial u}{\partial r}+\left(\frac{\partial u}{\partial r}\right)^2\right)\right)\left(\frac{\partial u}{\partial r}-\frac{u}{S+r}\right)\Bigg|_{r=0},$$
$$q_w=-\left(\frac{\partial T}{\partial r}\right)_{r=0},h_m=-\left(\frac{\partial C}{\partial r}\right)_{r=0}. \tag{18}$$

Using Eq. (7) in Eqs. 17 and 18, we obtain Eqs. 19–21 as follows:

$$Re_s^{-1/2}C_f=F''(0)-\frac{\varpi}{6}\left(-\frac{3}{\varsigma}F''(0)+\frac{3}{\varsigma^2}F''(0)-\frac{1}{\varsigma^3}+F''(0)^3\right)-\frac{1}{\varsigma}, \tag{19}$$

$$Re_s^{-1/2}Nu_n = -\left(\left(1+\frac{4}{3}R_d\right)\right)\theta'(0), \tag{20}$$

$$Re_s^{-1/2}Sh_n = -\varphi'(0) \tag{21}$$

3. Numerical procedure

The dimensionless differential equations 13–16 are transformed into first order differential equation as initial value problem and the procedure are defined in detail. The convergent criteria of the present model is 10^{-6} and the finite range is considered in $\Upsilon_\infty = 10$. The finite range $\Upsilon_\infty = 10$ are shown correct results and satisfied the numerical results asymptotically. The procedure are mentioned in detail as below:

$$Y(1) = F(\Upsilon);\ Y(2) = F'(\Upsilon); Y(3) = F''(\Upsilon);\ Y(4) = F'''(\Upsilon);\ YY1 = F''''(\Upsilon);$$

$$YY1 = \left(1-\left(\frac{\varpi}{2}\right)\left(\frac{Y(2)Y(2)}{2}+Y(3)Y(3)-2\frac{Y(3)Y(2)}{\Upsilon+\varsigma}\right)\right)^{-1}\left(-\frac{Y(2)-2\varsigma Y(1)Y(2)}{(\Upsilon+\varsigma)^3}-\left(\frac{\varpi}{2}\right)\left(\frac{4Y(2)Y(3)Y(4)}{2}+2Y(3)Y(4)Y(4)\right.\right.$$
$$-\frac{Y(2)Y(2)Y(2)}{(\Upsilon+\varsigma)^5}-\frac{2Y(3)Y(4)Y(3)}{\Upsilon+\varsigma}-\frac{2Y(2)Y(2)Y(4)}{(\Upsilon+\varsigma)^3}-\frac{3Y(2)Y(3)Y(3)}{(\Upsilon+\varsigma)^3}+\frac{3Y(2)Y(2)Y(3)}{(\Upsilon+\varsigma)^4}+\frac{Y(3)Y(3)Y(3)}{(\Upsilon+\varsigma)^2}$$
$$\left.-2\frac{Y(3)Y(3)Y(2)}{\Upsilon+\varsigma}\right)+\frac{2Y(4)+2\varsigma(Y(1)Y(4)-Y(3)Y(2))}{\Upsilon+\varsigma}-\frac{2\varsigma Y(2)Y(2)+Y(3)+2\varsigma Y(1)Y(3)}{(\Upsilon+\varsigma)^2}\Bigg);$$

$$Y(5) = \theta(\Upsilon);\ Y(6) = \theta'(\Upsilon); YY2 = \theta''(\Upsilon);$$

$$YY2 = \frac{Pr}{\left(1+\frac{4}{3}R\right)}\left(\frac{\varsigma}{\Upsilon+\varsigma}Y(6)Y(1)+(N_BY(8)Y(6)+N_TY(6)Y(6))+Ec\left(Y(3)Y(3)-\frac{2Y(2)Y(3)}{\Upsilon+\varsigma}+\frac{Y(2)Y(2)}{(\Upsilon+\varsigma)^2}\right.\right.$$
$$-\left(\frac{\varpi}{4}\right)\left(\frac{2Y(2)Y(2)Y(3)Y(3)}{(\Upsilon+\varsigma)^2}+Y(3)Y(3)Y(3)Y(3)+\frac{Y(2)Y(2)Y(2)Y(2)}{(\Upsilon+\varsigma)^4}-\frac{4Y(3)Y(3)Y(3)Y(2)}{\Upsilon+\varsigma}\right.$$
$$\left.\left.\left.-4\frac{Y(2)Y(2)Y(2)Y(3)}{(\Upsilon+\varsigma)^3}+4\frac{Y(2)Y(2)Y(3)Y(3)}{(\Upsilon+\varsigma)^2}\right)\right)\right)-\frac{\left(1+\frac{4}{3}R\right)}{Pr}\frac{1}{\Upsilon+\varsigma}Y(6);$$

$$Y(8) = \varphi'(\Upsilon); Y(7) = \varphi(\Upsilon); YY3 = \varphi''(\Upsilon);$$

$$YY3 = -\left(\frac{\varsigma}{\Upsilon+\varsigma}Y(8)Y(1)+\frac{N_B}{N_T}\left(YY2+\frac{1}{\Upsilon+\varsigma}Y(6)\right)\right)-\frac{1}{\Upsilon+\varsigma}Y(8);$$

having boundary conditions are

$$Y0(1)-\omega;\quad Y0(2)-1;\quad Yinf(2);\ Yinf(3);\ \delta_1Y0(8)+1-Y0(7);$$

$$Yinf(5);\ Yinf(7);\ \delta Y0(6)+1-Y0(5);$$

$\widetilde{R}_1, \widetilde{R}_2, \widetilde{R}_3$ are the residual of current model and the system of differential equations are cracked by implementing the numerical

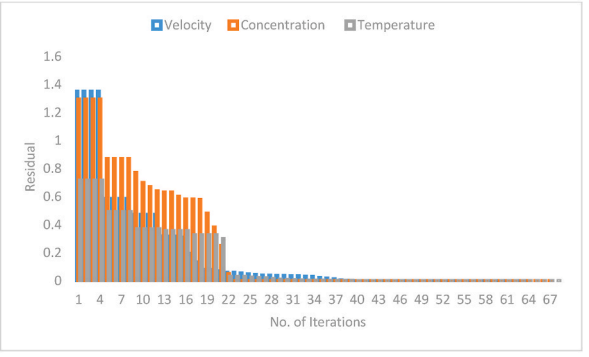

Fig. 1(b). Residual error of the present work.

scheme RK-4th order. The solution converge criteria defined that the tolerance error is less than 10^{-6}. Residuals are revealed as:

$$\widetilde{R}_1 = |Y_2(\infty) - \widehat{Y_2}(\infty)|;$$

$$\widetilde{R}_2 = |Y_5(\infty) - \widehat{Y_5}(\infty)|;$$

$$\widetilde{R}_3 = |Y_7(\infty) - \widehat{Y_7}(\infty)|;$$

Hence, $\widehat{Y_2}(\infty), \widehat{Y_5}(\infty), \widehat{Y_7}(\infty)$ are calculated boundary values. The residual error of the present work is highlighted in Fig. 1(b).

4. Results and discussion

The results of the concerning parameters: Eckert number (Ec), Brownian motion (N_B), Thermophoresis (N_T) and radiation (R_d) on the temperature ($\theta(\Upsilon)$) are presented in Figs. (2–5) for the both cases of suction/injection. Fig. 2 debated the influence of Eckert number on the temperature ($\theta(\Upsilon)$). The temperature increased due to a rise in the Eckert number. The higher Eckert number enhanced the kinetic energy, which then converted into internal energy. This internal energy counteracted the viscous stress of the fluid, ultimately leading to growth in the temperature. The difference of temperature ($\theta(\Upsilon)$) and Brownian motion (N_B) which presented in Fig. 3. The relation between temperature ($\theta(\Upsilon)$) and Brownian motion (N_B) have directly proportion. Brownian motion enriched which improved the temperature ($\theta(\Upsilon)$) because energy (K. E) increased the motion of the particle of the fluid ultimately, fluid temperature improved. Fig. 4 presented the impression of thermophoresis on the fluid temperature ($\theta(\Upsilon)$). The relationship with thermophoresis and fluid temperature ($\theta(\Upsilon)$) have directly proportion. Impression of radiation (R_d) on fluid temperature ($\theta(\Upsilon)$) exhibited in Fig. 5. Radiation improved fluid temperature ($\theta(\Upsilon)$) because stronger radiation is more heated the surface. Influence of curvature (ς) on fluid temperature ($\theta(\Upsilon)$) which revealed in Fig. 6. Temperature ($\theta(\Upsilon)$) revealed the curves declined by boosting values of curvature (ς) because surface become flat and temperature spread, so heat reduced. Influence of curvature (ς), thermophorsis (N_T), sutterby fluid (ϖ) and Brownian motion (N_B) on the concentration ($\varphi(\Upsilon)$) which exhibited in Figs. 7–10. Impression of curvature (ς) and concentration ($\varphi(\Upsilon)$) presented in Fig. (7). It is noted that concentration ($\varphi(\Upsilon)$) curves enriched due to boosting values of curvature (ς). Fig. 8 reported the influence of thermophorsis (N_T) on the concentration ($\varphi(\Upsilon)$). The concentration ($\varphi(\Upsilon)$) curves condensed by larger values of thermophorsis (N_T). Impression of sutterby fluid (ϖ) and fluid concentration ($\varphi(\Upsilon)$) presented in Fig. (9). It is noted that fluid concentration ($\varphi(\Upsilon)$) curves enriched due to boosting values of sutterby fluid (ϖ). Fig. (10) reported the influence of Brownian motion (N_B) on the fluid concentration ($\varphi(\Upsilon)$). The fluid concentration ($\varphi(\Upsilon)$) curves improved by larger values of Brownian motion (N_B). Table 1 stated the influence of Brownian motion (N_B), thermophoresis (N_T), sutterby fluid (ϖ), curvature (ς), Eckert number (Ec), radiation (R_d), Prandtl number (Pr), thermal slip (δ) and concentration slip (δ_1) on absolute value of $C_f Re^{1/2}$, $Nu_n Re^{-1/2}$ and $Sh_n Re^{-1/2}$. Nusselt number ($Nu_n Re^{-1/2}$) boosted up while sherwood number ($Sh_n Re^{-1/2}$) declined for larger values of Brownian motion (N_B) and skin friction remain constant. The relation between thermophoresis (N_T) and Nusselt number ($Nu_n Re^{-1/2}$) have inversely while with Sherwood number ($Sh_n Re^{-1/2}$) have directly. The values of sutterby fluid (ϖ) boosted which resist to increasing values of absolute

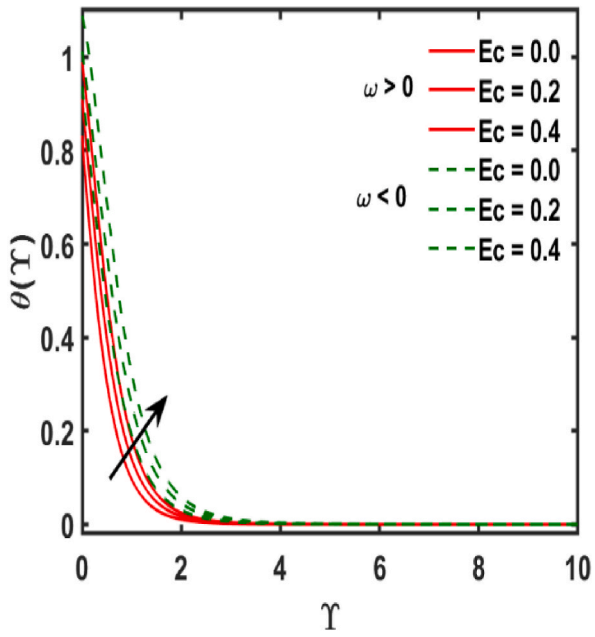

Fig. 2. Variation of Ec and $\theta(\Upsilon)$.

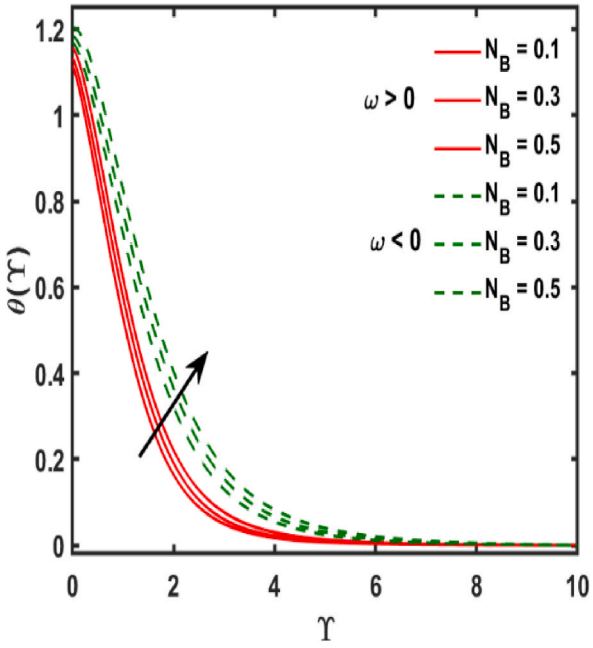

Fig. 3. Variation of N_B and $\theta(\Upsilon)$.

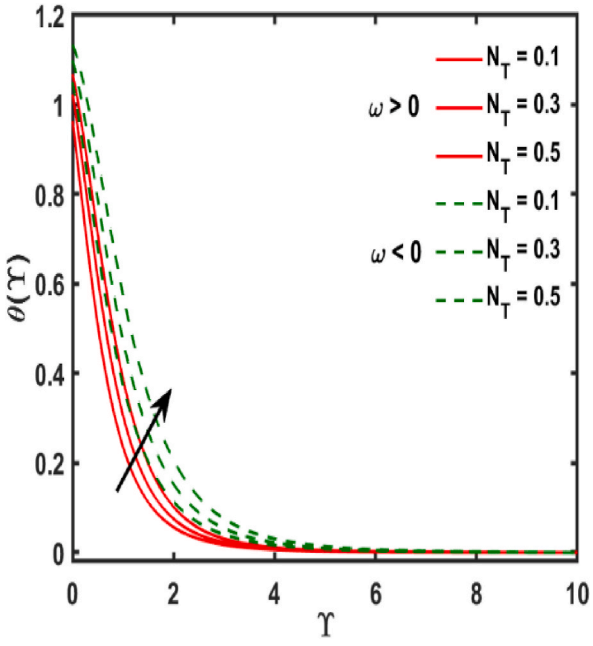

Fig. 4. Variation of N_T and $\theta(\Upsilon)$.

value of skin friction ($C_f Re^{1/2}$). Because, viscosity enriched due to increment in sutterby fluid increase ultimately, skin friction increased at the surface. Variation of Nusselt number ($Nu_n Re^{-1/2}$) and sutterby fluid (ϖ) presented in Table 1. The relation between Nusselt number ($Nu_n Re^{-1/2}$) and sutterby fluid (ϖ) have found to be directly which inversely relationship with Sherwood ($Sh_n Re^{-1/2}$) because heat transfer improved and mass transfer reduced. The curvature (ς) increased which increased the absolute value of skin friction ($C_f Re^{1/2}$) because the values of curvature increase which surface become flat so skin friction increased. The curvature (ς) and Nusselt number ($Nu_n Re^{-1/2}$) found to be inversely relation. The surface become flat and heat reduced due to larger values of curvature (ς) while same behavior found for Sherwood ($Sh_n Re^{-1/2}$) have increasing. Relationship between Eckert number (Ec) and Nusselt

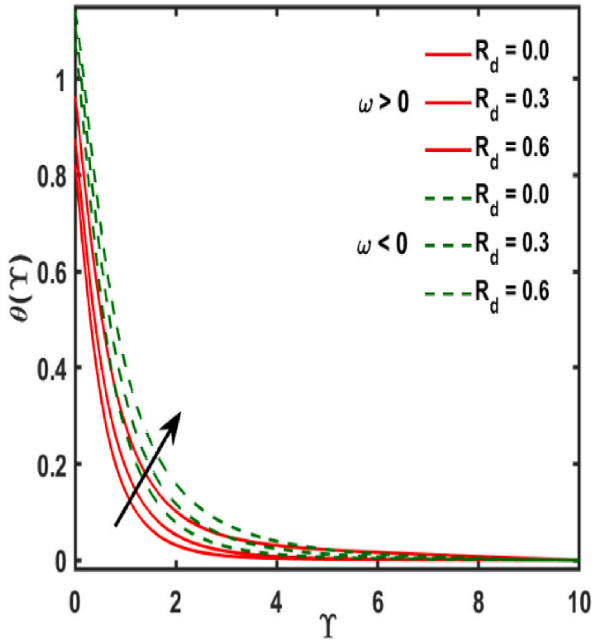

Fig. 5. Variation of R_d and $\theta(\Upsilon)$.

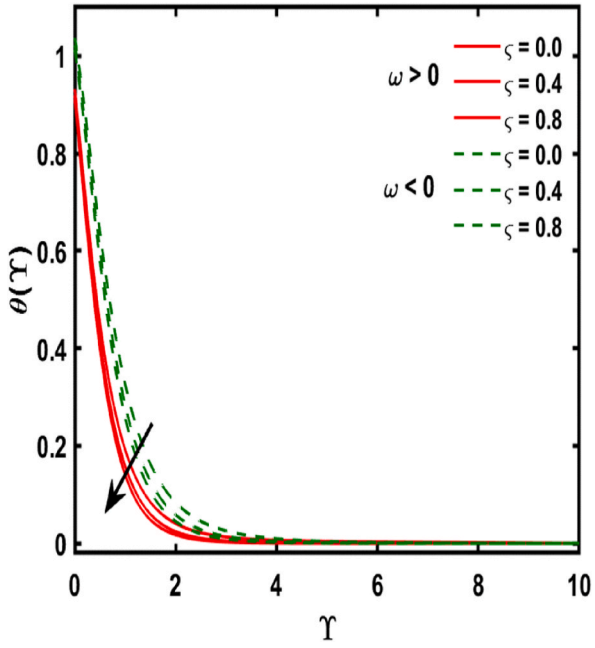

Fig. 6. Variation of ς and $\theta(\Upsilon)$.

number ($Nu_nRe^{-1/2}$) have opposite but same relationship between Eckert number (Ec) and Sherwood ($Sh_nRe^{-1/2}$). Relationship between radiation (R_d) and Nusselt number ($Nu_nRe^{-1/2}$) have directly but same relationship between radiation (R_d) and sherwood ($Sh_nRe^{-1/2}$) have increasing. Radiation improved which boosted up the heat transfer rate and also boosted up mass transfer. The heat transfer enhanced due to greater values of Prandtl number (Pr) while mass transfer condensed as well as Prandtl number (Pr) increased. Relationship between thermal slip (δ) and Nusselt number ($Nu_nRe^{-1/2}$) have opposing behavior. The relationship between thermal slip (δ) and sherwood ($Sh_nRe^{-1/2}$) have opposing behavior. The concentration slip (δ_1) increased which declined the Nusselt number ($Nu_nRe^{-1/2}$). The concentration slip (δ_1) increased which declined the sherwood ($Sh_nRe^{-1/2}$). Table 2 shows our results compared to

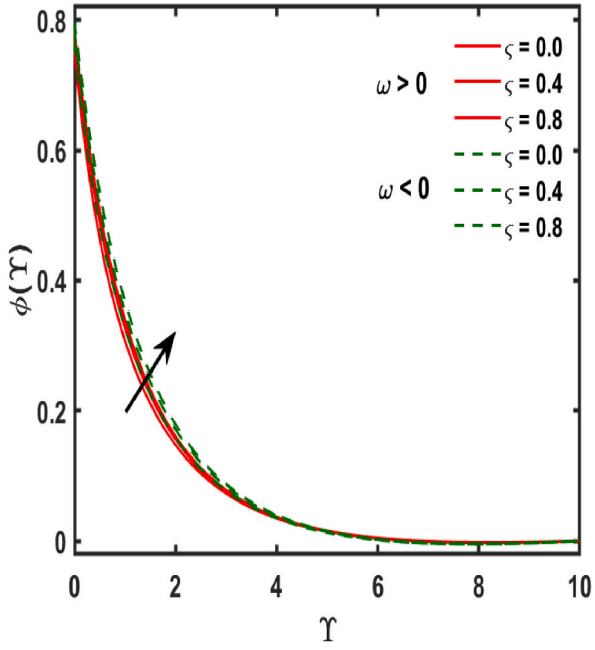

Fig. 7. Variation of ς and $\varphi(\Upsilon)$.

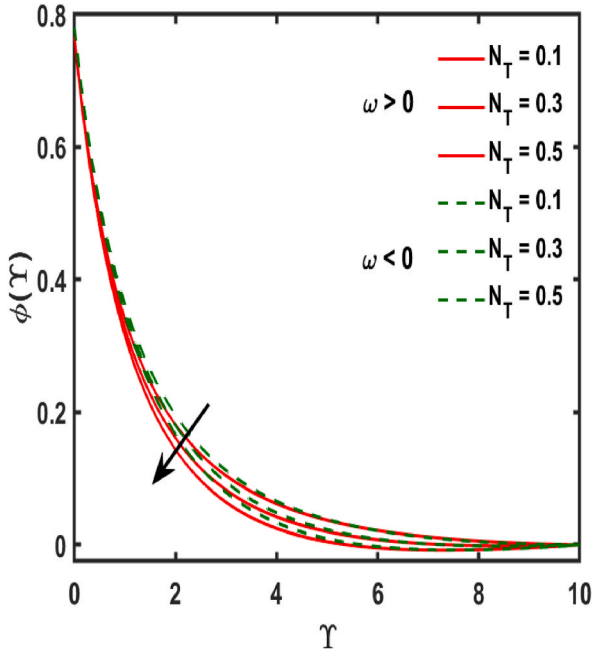

Fig. 8. Variation of N_T and $\varphi(\Upsilon)$.

Okechi et al. [41], with our results being more accurate and approaching literature more closely.

5. Final remarks

Steady incompressible two-dimensional satterby nanofluid flow at a curved surface is considered. Thermal and concentration slip phenomena under radiation effects are taken into account. The thermophoresis and Brownian motion process were exhibited on the curved surface. The numerical solution of the specified mathematical model is obtained using the built-in bvp4c tool in MATLAB. The effects of various parameters related to the system of ordinary differential equations are illustrated in the graphs and tabular form. The

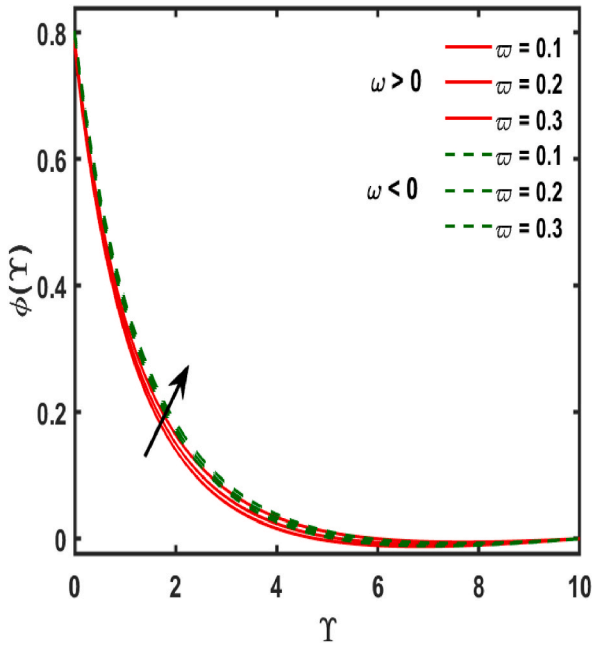

Fig. 9. Variation of ϖ and $\varphi(\Upsilon)$.

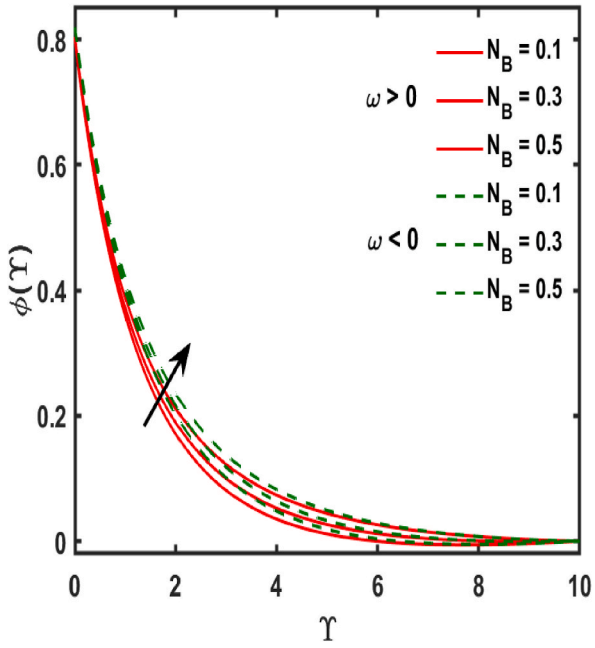

Fig. 10. Variation of N_B and $\varphi(\Upsilon)$.

main results are presented below:

- Temperature boosted up for improving the Eckert number. The Eckert number increased which improved the K. E. The K. E transformed into to I. E which work against the viscous of fluid stress ultimately, temperature of fluid boosted.
- The relation between fluid temperature ($\theta(\Upsilon)$) and Brownian motion (N_B) have directly proportion. Brownian motion enriched which improved the fluid temperature ($\theta(\Upsilon)$) because energy (K. E) increased the motion of the particle of the fluid ultimately, fluid temperature improved.

Table 1
Variation of physical parameters on the $C_f Re^{1/2}$, $Nu_n Re^{-1/2}$ and $Sh_n Re^{-1/2}$.

N_B	N_T	ϖ	ς	Ec	R_d	Pr	δ	δ_1	$C_f Re^{1/2}$	$Nu_n Re^{-1/2}$	$Sh_n Re^{-1/2}$
0.1	0.4	0.5	4.0	0.2	0.5	3.0	0.3	0.2	−5.2993	1.1243	0.4209
0.3									−5.2993	1.1329	0.1597
0.5									−5.2993	1.1479	−0.1182
0.7									−5.2993	1.2141	−0.4622
0.5	0.2								−5.2993	1.4653	−1.2139
	0.4								−5.2993	1.1479	−0.1182
	0.6								−5.2993	1.0424	0.1633
	0.8								−5.2993	0.9809	0.2869
	0.4	0.1							−5.1626	0.5609	0.4818
		0.3							−5.2543	0.6239	0.4188
		0.5							−5.2993	1.1479	−0.1182
		0.7							−5.8488	1.3787	−0.3160
		0.5	3.0						−4.3645	1.5110	−0.0742
			4.0						−5.2993	1.1479	−0.1182
			5.0						−6.3437	1.0784	−0.1358
			6.0						−7.3174	1.0925	−0.1620
			4.0	0.0					−5.2993	1.2890	−0.2309
				0.2					−5.2993	1.1479	−0.1182
				0.4					−5.2993	1.0077	−0.0962
				0.6					−5.2993	0.8685	0.0451
				0.2	0.0				−5.2993	0.6345	−2.6361
					0.5				−5.2993	1.1479	−0.1182
					1.0				−5.2993	1.2367	0.0775
					1.5				−5.2993	1.3166	0.1831
					0.5	2.0			−5.2993	0.8380	0.1096
						3.0			−5.2993	1.1479	−0.1182
						4.0			−5.2993	1.4382	−0.3428
						5.0			−5.2993	4.3908	−2.6361
						3.0	0.1		−5.2993	1.1479	−0.1182
							0.3		−5.2993	1.0677	−0.0911
							0.5		−5.2993	1.0360	−0.0802
							0.7		−5.2993	1.0057	−0.0706
							0.1	0.1	−5.2993	1.1479	−0.1182
								0.2	−5.2993	1.1481	−0.1165
								0.3	−5.2993	1.1480	−0.1142
								0.4	−5.2993	1.1479	−0.1119

Table 2
Comparing the results of our analysis to the literature, assuming the other physical parameters are zero.

ς	Current analysis	Okechi et al. [41]
5.00	1.4206532	1.41960
10.00	1.3454691	1.34670
20.00	1.3109850	1.31350
30.00	1.2997415	1.30280
40.00	1.2942970	1.29750
50.00	1.2908963	1.29440
100.0	1.2844968	1.28810
200.0	1.2812471	1.28500
1000.0	1.2783552	1.28180

- Temperature ($\theta(\Upsilon)$) revealed the curves declined by boosting values of curvature (ς) because surface become flat and temperature spread, so heat reduced.
- Radiation improved fluid temperature ($\theta(\Upsilon)$) because stronger radiation is more heated the surface. It is noted that fluid concentration ($\varphi(\Upsilon)$) curves enriched due to boosting values of sutterby fluid (ϖ).
- The heat and mass transfer in case of section achieved lesser than that of injection case.

Consent for publication

Consent for publication ensures that authors give explicit, informed permission to publish their data and maintain ethical standards.

Availability of data and material

Data will be made available on request.

CRediT authorship contribution statement

Nadeem Abbas: Writing – review & editing, Writing – original draft, Methodology, Conceptualization. **Wasfi Shatanawi:** Validation, Supervision, Investigation. **Fady Hasan:** Writing – original draft, Methodology, Formal analysis, Data curation. **Zead Mustafa:** Validation, Methodology, Formal analysis, Data curation.

Declaration of competing interest

All the authors have no declaration of interest in the manuscript.

Acknowledgements

Authors would like to thank the Prince Sultan University for their support through the TAS research lab. The authors extend their appreciation to the TAS Lab at the Prince Sultan University for funding this work through SEED Project under grant number SEED-CHS-2024-163.

References

[1] J.L. Sutterby, Laminar converging flow of dilute polymer solutions in conical sections: Part I. Viscosity data, new viscosity model, tube flow solution, AIChE J. 12 (1) (1966) 63–68.
[2] N.S. Akbar, S. Nadeem, Convective heat transfer of a Sutterby fluid in an inclined asymmetric channel with partial slip, Heat Tran. Res. 45 (3) (2014).
[3] S. Ahmad, M. Farooq, M. Javed, A. Anjum, Double stratification effects in chemically reactive squeezed Sutterby fluid flow with thermal radiation and mixed convection, Results in physics 8 (2018) 1250–1259.
[4] M.I. Khan, S. Qayyum, T. Hayat, A. Alsaedi, Stratified flow of Sutterby fluid with homogeneous-heterogeneous reactions and Cattaneo-Christov heat flux, Int. J. Numer. Methods Heat Fluid Flow. 29 (8) (2019) 2977–2992.
[5] T. Sajid, S. Tanveer, Z. Sabir, J.L.G. Guirao, Impact of activation energy and temperature-dependent heat source/sink on Maxwell–Sutterby fluid, Math. Probl Eng. 2020 (2020) 1–15.
[6] F. Mabood, J. Mackolil, B.S.E.P. Mahanthesh, A. Rauf, S.A. Shehzad, Dynamics of Sutterby fluid flow due to a spinning stretching disk with non-Fourier/Fick heat and mass flux models, Appl. Math. Mech. 42 (9) (2021) 1247–1258.
[7] S. Abdal, I. Siddique, S. Afzal, S. Sharifi, M. Salimi, A. Ahmadian, An analysis for variable physical properties involved in the nano-biofilm transportation of sutterby fluid across shrinking/stretching surface, Nanomaterials 12 (4) (2022) 599.
[8] A. Hanif, Z. Abbas, S. Khaliq, Rheological impact of Sutterby fluid in isothermal forward roll coating process: a theoretical study, J. Plast. Film Sheeting 39 (1) (2023) 115–133.
[9] I. Hussain, W.A. Khan, M. Tabrez, M. Irfan, Dynamics of stratifications and magnetic dipole for radiative flow of ferromagnetic Sutterby fluid, ZAMM-Journal of Applied Mathematics and Mechanics/Zeitschrift für Angewandte Mathematik und Mechanik 103 (3) (2023) e202200226.
[10] Z. Hussain, W.A. Khan, M. Ali, H. Shahid, M. Irfan, Simultaneous features of nonuniform heat sink/source and activation energy in entropy optimized flow of Sutterby fluid subject to thermal radiation, Int. J. Mod. Phys. B. 37 (21) (2023) 2350208.
[11] S.I. Abdelsalam, A. Magesh, P. Tamizharasi, A.Z. Zaher, Versatile response of a Sutterby nanofluid under activation energy: hyperthermia therapy, Int. J. Numer. Methods Heat Fluid Flow (2023).
[12] B. Ishtiaq, S. Nadeem, J. Alzabut, Effects of variable magnetic field and partial slips on the dynamics of Sutterby nanofluid due to biaxially exponential and nonlinear stretchable sheets, Heliyon 9 (7) (2023) e17921.
[13] R. Raza, R. Naz, S.I. Abdelsalam, Microorganisms swimming through radiative Sutterby nanofluid over stretchable cylinder: hydrodynamic effect, Numer. Methods Part. Differ. Equ. 39 (2) (2023) 975–994.
[14] L.J. Crane, Boundary layer flow on a circular cylinder moving in a fluid at rest, Zeitschrift für angewandte Mathematik und Physik ZAMP 23 (1972) 201–212.
[15] K. Vajravelu, J.R. Cannon, Fluid flow over a nonlinearly stretching sheet, Appl. Math. Comput. 181 (1) (2006) 609–618.
[16] M. Sajid, N. Ali, T. Javed, Z. Abbas, Stretching a curved surface in a viscous fluid, Chin. Phys. Lett. 27 (2) (2010) 024703.
[17] Z. Abbas, M. Naveed, M. Sajid, Heat transfer analysis for stretching flow over a curved surface with magnetic field, J. Eng. Thermophys. 22 (2013) 337–345.
[18] N.S. Akbar, A. Ebaid, Z.H. Khan, Numerical analysis of magnetic field effects on Eyring-Powell fluid flow towards a stretching sheet, J. Magn. Magn Mater. 382 (2015) 355–358.
[19] K.M. Sanni, S. Asghar, M. Jalil, N.F. Okechi, Flow of viscous fluid along a nonlinearly stretching curved surface, Results Phys. 7 (2017) 1–4.
[20] R.S. Saif, T. Muhammad, H. Sadia, R. Ellahi, Hydromagnetic flow of Jeffrey nanofluid due to a curved stretching surface, Phys. Stat. Mech. Appl. 551 (2020) 124060.
[21] R.N. Kumar, R.P. Gowda, M.M. Alam, I. Ahmad, Y.M. Mahrous, M.R. Gorji, B.C. Prasannakumara, Inspection of convective heat transfer and KKL correlation for simulation of nanofluid flow over a curved stretching sheet, Int. Commun. Heat Mass Tran. 126 (2021) 105445.
[22] M.M. Bhatti, S.I. Abdelsalam, Scientific breakdown of a ferromagnetic nanofluid in hemodynamics: enhanced therapeutic approach, Math. Model Nat. Phenom. 17 (2022) 44.
[23] Y. Nawaz, M.S. Arif, K. Abodayeh, An unconditionally stable third order scheme for mixed convection flow between parallel plates with oscillatory boundary conditions, Int. J. Numer. Methods Fluid. 95 (6) (2023) 937–953.
[24] N. Abbas, W. Shatanawi, A.M. Taqi, Thermodynamic study of radiative chemically reactive flow of induced MHD sutterby nanofluid over a nonlinear stretching cylinder, Alex. Eng. J. 70 (2023) 179–189.
[25] N. Abbas, W. Shatanawi, K. Abodayeh, T.A. Shatnawi, Comparative analysis of unsteady flow of induced MHD radiative Sutterby fluid flow at nonlinear stretching cylinder/sheet: variable thermal conductivity, Alex. Eng. J. 72 (2023) 451–461.
[26] K. Sakkaravarthi, P.B.A. Reddy, Entropy optimization of MHD hybrid nanofluid flow through a curved stretching sheet with thermal radiation and heat generation: semi-analytical and numerical simulations, Proc. IME E J. Process Mech. Eng. 237 (2) (2023) 138–148.
[27] S.I. Abdelsalam, M.M. Bhatti, Unraveling the nature of nano-diamonds and silica in a catheterized tapered artery: highlights into hydrophilic traits, Sci. Rep. 13 (1) (2023) 5684.
[28] J. Buongiorno, Convective Transport in Nanofluids, 2006, pp. 240–250.
[29] P. Rana, R. Bhargava, O.A. Bég, Finite element simulation of unsteady magneto-hydrodynamic transport phenomena on a stretching sheet in a rotating nanofluid, Proc. Inst. Mech. Eng. - Part N J. Nanoeng. Nanosyst. 227 (2) (2013) 77–99.

[30] M. Goyal, R. Bhargava, Finite element solution of double-diffusive boundary layer flow of viscoelastic nanofluids over a stretching sheet, Comput. Math. Math. Phys. 54 (2014) 848–863.
[31] N.S. Akbar, Peristaltic flow of a Sutterby nanofluid with double-diffusive natural convection, J. Comput. Theor. Nanosci. 12 (8) (2015) 1546–1552.
[32] T. Hayat, S. Ahmad, M.I. Khan, A. Alsaedi, Modeling chemically reactive flow of sutterby nanofluid by a rotating disk in presence of heat generation/absorption, Commun. Theor. Phys. 69 (5) (2018) 569.
[33] M. Sohail, R. Naz, Modified heat and mass transmission models in the magnetohydrodynamic flow of Sutterby nanofluid in stretching cylinder, Phys. Stat. Mech. Appl. 549 (2020) 124088.
[34] W.A. Khan, Z. Arshad, A. Hobiny, S. Saleem, A. Al-Zubaidi, M. Irfan, Impact of magnetized radiative flow of sutterby nanofluid subjected to convectively heated wedge, Int. J. Mod. Phys. B 36 (16) (2022) 2250079.
[35] S.I. Abdelsalam, A.Z. Zaher, On behavioral response of ciliated cervical canal on the development of electroosmotic forces in spermatic fluid, Math. Model Nat. Phenom. 17 (2022) 27.
[36] A. Aldabesh, A. Haredy, K. Al-Khaled, S.U. Khan, I. Tlili, Darcy resistance flow of Sutterby nanofluid with microorganisms with applications of nano-biofuel cells, Sci. Rep. 12 (1) (2022) 7514.
[37] Y. Nawaz, M.S. Arif, K. Abodayeh, M.U. Ashraf, M. Naz, A new explicit numerical scheme for enhancement of heat transfer in Sakiadis flow of micro polar fluid using electric field, Heliyon 9 (10) (2023) e20868.
[38] R. Raza, R. Naz, S.I. Abdelsalam, Microorganisms swimming through radiative Sutterby nanofluid over stretchable cylinder: hydrodynamic effect, Numer. Methods Part. Differ. Equ. 39 (2) (2023) 975–994.
[39] A.A. Khan, A. Arshad, R. Ellahi, S.M. Sait, Heat transmission in Darcy-Forchheimer flow of Sutterby nanofluid containing gyrotactic microorganisms, Int. J. Numer. Methods Heat Fluid Flow 33 (1) (2023) 135–152.
[40] S.I. Abdelsalam, A.M. Alsharif, Y. Abd Elmaboud, A.I. Abdellateef, Assorted kerosene-based nanofluid across a dual-zone vertical annulus with electroosmosis, Heliyon 9 (5) (2023) e15916.
[41] N.F. Okechi, M. Jalil, S. Asghar, Flow of viscous fluid along an exponentially stretching curved surface, Results Phys. 7 (2017) 2851–2854.